

Synthesis and Characterization of Well-Defined, Tadpole-Shaped Polystyrene with a Single Atom Junction Point

Fan Zhang, ** Roderic P. Quirk, ** Selim Gerislioglu, ** Chrys Wesdemiotis, **, ** Selemon Bekele, ** Mesfin Tsige, ** Yung P. Koh, ** Sindee L. Simon, ** and Mark D. Foster**, ** and Mark D. Foster**, **

[†]Department of Polymer Science and [‡]Department of Chemistry, The University of Akron, Akron, Ohio 44325, United States §Department of Chemical Engineering, Texas Tech University, Lubbock, Texas 79409, United States

Supporting Information

ABSTRACT: An efficient method for synthesis of welldefined, well-characterized, tadpole-shaped polystyrene with a single atom junction point that is optimal for the study of dynamics has been developed using anionic polymerization, silicon chloride linking chemistry, and metathesis ring closure. The difunctional macromolecular linking agent, ω -methyldichlorosilylpolystyrene, was formed by reacting sec-butyllithium-initiated poly(styryl)lithium with excess (30×) methyltrichlorosilane to eliminate formation of linear dimer and three-arm star polystyrene. The asymmetric, three-arm,

star precursor was formed by linking excess \alpha-4-pentenylpoly(styryl)lithium (\alpha-PSLi) with the macromolecular linking agent, and the excess \alpha-PSLi functionalized with ethylene oxide before termination with methanol to facilitate chromatographic separation. Cyclization of the three-arm, star precursor to form tadpole-shaped polystyrene was effected in methylene chloride at high dilution using the Grubbs first generation catalyst, bis(tricyclohexylphosphine)benzylidene ruthenium(IV) chloride. The tadpole product was uniquely characterized by MALDI-MS using peaks that appeared characteristically $28\ m/z$ units lower than those of the corresponding asymmetric, three-arm, star precursor, which corresponds to the loss of an ethylene unit. MD simulations find a smaller hydrodynamic volume for the tadpole-shaped PS as compared to the three-arm star precursor, in quantitative agreement with GPC results. Incorporating one cycle in the molecule, while leaving one chain end, leads to an increase in $T_{\rm g}$ of only 2.7 °C, much smaller than the increase of 13.6 °C seen when going from the linear chain to cyclic analog with no ends at all. The results are consistent with self-plasticization by free chain ends.

INTRODUCTION

The properties of polymers of nonlinear architecture such as star and cyclic chains can be strikingly different than those of linear analogues, ¹⁻³ both in bulk ⁴⁻⁶ and in thin films. ⁷⁻¹⁰ For example, the T_g 's of cyclic polystyrenes (PS) are substantially higher than those of linear analogues for degrees of polymerization < 400.^{2,11} Monteiro and co-workers¹² measured T_g 's for two types of linear PS (LPS), tadpole-shaped PS (TPS) and bicylic PS formed with a triazole junctions. One of the linear chains had conventional architecture while the other was a two arm star with a bifunctional triazole junction in the middle. They also reported that the $T_{\rm g}$ for their 10k TPS sits 1-2 °C below the $T_{\rm g}$ they expect for a cyclic analog based on comparison with $T_{\rm g}$ values for cyclics with various M reported by Hogen-Esch and co-workers 13 and sits ca. 6 $^{\circ}$ C above the $T_{\rm g}$ of the linear analog based on the Kanig-Ueberreiter equation.14

The linking chemistry they use introduces considerable heterogeneity into the chain chemistry, and the mobility around the junction point is limited. Floudas and co-workers 15 recently studied segmental dynamics for various multicyclic polystyrenes from Monteiro's group. They observed, generally, a linear increase in T_g with the number of segments adjacent to

the junctions, suggesting that the bulk dynamics are strongly dependent on the number of segments constrained by attachment to the junctions. Chains with more branching points are more structurally hindered. Strong effects of branching in star PS and cyclization in cyclic PS on surface fluctuations of melts has also been identified by Foster and coworkers. 8-10,16 In particular, Foster and co-workers 9 found that confinement effects set in for surface fluctuations of thin melt films of cyclic polystyrene at higher film thickness (both in absolute thickness and relative to R_g) than for films of linear analogues. Those authors hypothesized that more efficient packing of the cyclic chains at the substrate is responsible for this. Therefore, it is of interest to consider how such confinement effects may differ when the architecture of the chain is between those of cyclic and linear, such as for a tadpole-shaped polymer, which may be thought of as a macrocyclic polymer with a linear tail attached. Takano et al. 17 have reported that tadpole-shaped polystyrene shows a terminal relaxation that is slower than those of either the

Received: June 28, 2018 Revised: October 15, 2018 Published: November 19, 2018

Scheme 1. Reaction Route for the Synthesis of Tadpole-Shaped Polystyrene

component macrocyclic ring or linear chain and also slower than for blends in which macrocyclic and linear components are mixed. However, systematic study of tadpole-shaped polymers has been limited by the availability of molecules with well-defined structures.

Syntheses of tadpole-shaped polymer have been reported by several groups. Deffieux et al. ¹⁸ have proposed a method to synthesize tadpole-shaped polymers based on a unimolecular "end-to-end" coupling reaction of a heterodifunctional linear polymer precursor. A high molecular weight species was observed in the SEC chromatogram of the product, which was formed by intermolecular coupling of a small fraction of chains. Tezuka et al. ¹⁹ have reported an "electrostatic self-assembly and covalent fixation" process to synthesize tadpole-shaped polymers. They reported that the tadpole-shaped polymer was obtained in quantitative yield with a polydispersity of 1.27. Jérome and co-workers ²⁰ have tested a strategy for the synthesis of tadpole-shaped polyesters, which relied on the intramolecular photochemical cyclization of unsaturated acrylic units at both ends of precursor chains. These precursor chains were synthesized using ring-opening polymerization initiated

by a cyclic tin alkoxide. The molecular weight distribution of the rings was broad (PDI: 1.45) and the breadth of the distribution was ascribed to the nature of ring-opening polymerization. Shi et al.²¹ have reported a "click" synthetic route to obtain a tadpole-shaped copolymer. They first synthesized a linear acetylene-terminated poly(N-isopropylacrylamide)-b-PS precursor with an azido side group anchored at the junction between the two blocks. Intramolecular cyclization was then carried out to produce the tadpole-shaped block copolymer using "click" chemistry (Azide-alkyne Huisgen cycloaddition) under high dilution. By this method they synthesized a tadpole-shaped block copolymer with a narrow molecular weight distribution (PDI: 1.03) in a yield of 60%. Takano et al. 22 have synthesized tadpole-shaped polystyrene using a coupling reaction between ring polystyrene with two pendant diphenylethylene groups and linear poly-(styryl)lithium. The crude coupling product was a mixture of unreacted linear tail polymer, single-tail tadpole polymer, and twin-tail tadpole polymer.²² Precipitational fractionation was used to obtain single-tail tadpole-shaped polymer with high purity in 11% yield. These reported syntheses provided

tadpole-shaped polymers with relatively large and polar junction points (not a single atom), which we conjecture could affect the molecular dynamics.²³ In addition, these procedures generally required extra purification steps such as multiple fractionations and HPLC. In general, the molecular characterization of these tadpole polymers was limited. Therefore, development of an efficient strategy for synthesizing well-defined, tadpole-shaped polymers with single atom junction point is still a significant challenge.

The development of a multistep method combining anionic polymerization, silicon chloride linking chemistry, and metathesis ring closure has provided efficient procedures for synthesizing well-defined macrocycles^{24,25} and eight-shaped polystyrenes.²⁶ Living anionic polymerization is useful to prepare well-defined α - and ω -functionalized polymers. ^{27,28} Fetters and Bauer¹ and Hadjichristidis³ have shown that silicon chloride linking chemistry is one of the best methods to synthesize a variety of star-branched polymers with control over molecular weight and with narrow molecular weight distributions. Fetters and Pennisi, 29 Mays, 30 and Mays and coworkers³¹ have developed methods to synthesize asymmetric star copolymers using anionic polymerization and silicon chloride linking chemistry. Metathesis ring closure has been shown to be one of the best methods to make macrocycles from divinyl precursors; 24-26,32 thus it should be possible to prepare tadpole-shaped polymers using an asymmetric, threearm, star polymer with two vinyl chain-end groups as a precursor for metathesis ring-closure. On the basis of these precedents, here we present an efficient approach to synthesize well-defined, tadpole-shaped polystyrene by a combination of living alkyllithium-initiated anionic polymerization, silicon chloride linking chemistry, and metathesis ring closure, as shown in Scheme 1.

EXPERIMENTAL SECTION

Materials. Benzene (99%, EMD), styrene (99%, Aldrich), diethyl ether (EMD, 99%), and THF (>95%, Fisher Scientific) were purified as previously reported.^{24,33} 5-Bromo-1-pentene (95%, Aldrich) was stirred over calcium hydride, degassed three times, and fractionally distilled under vacuum into a graduated ampule, followed by flamesealing from the vacuum line. Methyltrichlorosilane (99%, Aldrich) was placed into a stopcock-sealed flask containing calcium hydride in the drybox, stirred overnight on the vacuum line, degassed and fractionally distilled under vacuum into a graduated ampule followed by flame-sealing. Lithium metal (stabilized, 1% Na, FMC) was stored in the drybox and used without further purification. Methanol (>99.8%, Fisher Scientific) was degassed on the vacuum line before distilling into an ampule followed by flame-sealing. Methylene chloride (>99%, Fisher Scientific) was stirred over calcium hydride, degassed, and distilled into a stopcock-sealed flask with a Rotoflo stopcock. Bis(tricyclohexylphosphine)benzylidene ruthenium(IV) chloride (97%, Aldrich) was dissolved in purified methylene chloride and transferred into a stopcock-sealed ampule in the drybox. The ampule was then degassed on the vacuum line and flame-sealed.

Synthesis of ω-Methyldichlorosilylpolystyrene (2). All polymerizations were conducted in all-glass apparatuses using standard high vacuum techniques. A 150 mL, glass reactor equipped with a septum-sealed side arm, ampules of styrene (5 mL, 4.55 g, 43.7 mmol), methanol (~2 mL), and an empty storage ampule with a stopcock was connected to the high vacuum line. *sec*-Butyllithium (1.9 mL, 2.27 mmol) was added into the reactor through the side arm using a gastight syringe under a flowing nitrogen atmosphere. After flame-sealing the side arm, benzene (100 mL) was vacuum distilled into the reactor. The reactor was then flame-sealed from the vacuum line and the break-seal of the styrene ampule was smashed. The reactor was placed in a water bath at 25 °C for 2 h, and

then 35 mL of the poly(styryl)lithium (1) solution was transferred into the stopcock-sealed storage ampule which was then flame-sealed from the reactor. The remaining poly(styryl)lithium (1) was quenched with methanol for characterization.

A 250 mL, Morton-creased, glass reactor equipped with ampules of poly(styryl)lithium solution (35 mL, 0.8 mmol), methyltrichlorosilane (2.9 mL, 24 mmol), benzene (20 mL), an empty storage ampule, and a Teflon stir bar was connected to the high vacuum line. Benzene (15 mL) was distilled into the reactor, and the reactor was separated from the vacuum line by flame-sealing. The break-seal of the methyltrichlorosilane ampule was broken, and the solution was stirred at 0 °C for 10 min. The break-seal of the poly(styryl)lithium (1) solution was then broken, and the solution was slowly added to the methyltrichlorosilane solution by adjusting the stopcock. The reactor was reconnected to the vacuum line after decolorization of the solution. The solvent was removed by three freeze-dry processes using benzene as solvent and then the reactor was flame-sealed from the vacuum line. The break-seal of the benzene ampule was broken and the resulting solution was transferred into the storage ampule and flame-sealed. The product was 0.8 mmol in benzene.

Synthesis of 5-Lithio-1-pentene. A 150 mL, Morton-creased, glass reactor equipped with a break-seal, a septum-sealed side arm and ampules of diethyl ether (20 mL), 5-bromo-1-pentene (6.5 mL, 0.055 mol), and a medium porosity fritted glass filter connected to an empty ampule was transferred into the drybox. Lithium (3.6 g, 0.52 mol) was added to the reactor through the side arm which was then plugged with a rubber septum. The reactor was removed from the drybox and connected to the vacuum line through a break-seal. After flame-sealing the side arm, heptane (50 mL) was distilled into the reactor and then the break-seal of the 5-bromo-1-pentene ampule was smashed. The mixture was stirred for 3 days at room temperature, and then the reactor was cooled to 0 $^{\circ}\text{C}$ with an ice—water bath. The break-seal of the diethyl ether ampule was smashed, and the mixture was stirred for another 24 h at 0 °C. The reactor was reconnected to the vacuum line through a break-seal. The break-seal was smashed and the solvent was stripped off through the vacuum line to remove diethyl ether from the reactor. Another batch of heptane (~50 mL) was distilled into the reactor, and the mixture was filtered into the empty ampule through the fritted glass filter. The reactor was rinsed by back-distilling heptane using an isopropyl alcohol/dry ice cooling bath and transferring back through the filter. The ampule containing this functionalized initiator solution was then flame-sealed from the reactor and transferred into the drybox. The initiator solution was diluted with heptane (~50 mL) and distributed into two crimp-cap bottles and sealed. The concentration of the 5-lithio-1-pentene initiator was determined using double titration to be 0.24 M.3

Synthesis of Asymmetric, Three-arm, Star Polystyrene (4). A 150 mL, Morton-creased glass reactor equipped with a septum-sealed side arm, ampules of styrene (5.5 mL, 5 g, 48 mmol), THF (1 mL, 12.3 mmol), ω -methyldichlorosilylpolystyrene (2) solution (0.8 mmol in benzene), ethylene oxide (1 mL in 5 mL of benzene, 20 mmol), and methanol (~2 mL) was connected to the vacuum line. The 5-lithio-1-pentene initiator (10.5 mL, 2.52 mmol) was injected into the reactor via the side arm using a gastight syringe under a flowing nitrogen atmosphere followed by flame-sealing of the side arm under high vacuum. Then benzene (100 mL) was distilled into the reactor cooled with a dry ice/isopropyl alcohol bath before it was removed from the line by flame-sealing. The break-seals of the THF and styrene ampules were smashed sequentially after the reactor was warmed to room temperature. The reactor was cooled to 0 °C and stirred for 3 h. An aliquot of the α -4-pentenylpoly(styryl)lithium (α -PSLi, 3) solution was transferred into an empty ampule equipped with a methanol ampule, flame-sealed from the vacuum line, and later quenched using methanol for characterization. The break-seal of the ω -methyldichlorosilylpolystyrene (2) ampule was smashed, and the mixture was stirred at 0 °C for 24 h. The break-seal of the ethylene oxide ampule was smashed, and the mixture was stirred for 10 min. The methanol ampule break-seal was then smashed, and all of the solvent was removed using a rotary evaporator. The crude product was dissolved in toluene (~2 mL) and precipitated into methanol

(~40 mL). The asymmetric, three-arm, star polystyrene (4) was purified by silica gel chromatography using toluene as eluent. The powder was dried in a high vacuum oven overnight before characterization using ¹H NMR, SEC, and MALDI-ToF mass spectrometry (MALDI-MS).

Synthesis of Tadpole-Shaped Polystyrene (5). The asymmetric, three-arm, star polystyrene (4, 400 mg, 0.067 mmol; M_n = 6000 g/mol) and bis(tricyclohexylphosphine)benzylidineruthenium-(IV) chloride (123 mg, 0.15 mmol) were each dissolved in dichloromethane (20 mL) and distributed into separate ampules with stopcocks in the drybox. The ampules were then taken out of the drybox and connected to the vacuum line. Both solutions were degassed using three freeze-pump-thaw cycles in a liquid nitrogen bath and were then removed from the vacuum line by flame-sealing. A 2 L glass reactor equipped with the two ampules was connected to the vacuum line, and dichloromethane (1 L) was distilled into the reactor by vacuum distillation. The reactor was then removed from the vacuum line by flame-sealing and warmed to room temperature. The break-seals of the asymmetric, three-arm, star polystyrene (4) and the ruthenium catalyst ampules were smashed sequentially. The mixture was stirred at 40 °C for 24 h before oxygen was bubbled through the solution for 30 min to deactivate the catalyst. After removing the solvent using a rotary evaporator, the residual catalyst was removed using alumina (neutral, Sigma-Aldrich) column chromatography with toluene as eluent. The product was dissolved in 10 mL of toluene, precipitated into methanol, and dried in a high vacuum oven overnight before characterization using ¹H NMR, SEC, and MALDI-

Molecular Dynamics Simulations. Molecular dynamics simulations were carried out for the star precursor PS and TPS. Both simulated chains have molecular weights exactly matching those of their experimental counterparts and were generated initially through the Discover module of Materials Studio 6.0 from Accelrys Inc. Each system consisted of 30 chains of the same molecular weight (PDI: 1.0) corresponding to 60 PS monomers. The systems were initially run in the NPT ensemble for 8 ns to determine the equilibrium average volume consistent with the target temperature density. Accordingly, the simulation box size for each system was set to a cubic box of around $71 \times 71 \times 71$ Å (with the dimensions changing less than 1 Å in each direction when the temperature was lowered from 550 to 510 K) for subsequent runs in the NVT ensemble for at least 10 ns. The systems were modeled with the OPLS-AA force field, which has been shown to capture structural and dynamical properties of PS that are consistent with experimental results. 39 The cutoff radius for the Lennard-Jones term was set to 12 Å. The particle-particle/ particle-mesh Ewald (PPPM) algorithm was used for the calculation of the Coulombic interactions. Both systems were further equilibrated for an additional 2 ns for the chains to diffuse through distances several times their end-to-end distance, and data were recorded every 2 ps during this 2 ns run for data analysis. Data from the last 1 ns of simulation were used for analysis. All simulations were carried out using the LAMMPS MD package 40 with an integration time step of 1

Characterization. Gel permeation chromatography (GPC) was performed using a Tosoh EcoSEC HLC-8320GPC instrument equipped with eight TSK gel columns (30 Å to 10000 Å) and a double detector system (refractive index and light scattering detectors). THF was used as the eluent with a flow rate of 1.0 mL/min at 30 °C. Samples were prepared in THF (5 mg/mL) and filtered through a 0.45 $\mu \rm m$ Teflon filter before injection. The intrinsic viscosities were obtained using a Viscotek viscometer, and the analyses were performed using Wyatt ASTRA software (version 5.63).

¹H NMR measurements were performed with a Varian 500 spectrophotometer (500 MHz) using 20 mg of product dissolved in 1 mL of CDCl₃ (D, 99.8%, Cambridge Isotopes). MALDI-MS data were obtained on a Bruker Ultraflex-III MALDI tandem time-of-flight (ToF/ToF) mass spectrometer (Bruker Daltonics, Bullerica, MA) equipped with a Nd: YAG laser (355 nm). Samples of 2-[(2E)-3-(4-tert-butylphenyl)-2-methylprop-2-enylidiene]malononitrile (20 mg/mL) (≥99%, Sigma-Aldrich, St. Louis, MO, USA) and silver

trifluoroacetate (10 mg/mL) (98%, Sigma-Aldrich, St. Louis, MO, USA) served as matrix and cationizing salt, respectively. Solutions of the matrix (20 mg/mL), cationizing salt (10 mg/mL), and the sample (10 mg/mL) were prepared in THF (Fisher, Fair Lawn, NJ). The matrix/sample/cationizing agent solutions were mixed at the ratio 10:2:1 (vol/vol/vol), and 0.5–1.0 μ L of the final mixture was applied to the MALDI sample target and allowed to dry at ambient conditions before spectral acquisition. This sample preparation protocol led to the formation of $[M+Ag]^+$ ions. Spectral acquisition was carried out in reflectron mode and ion source 1 (IS 1), ion source 2 (IS 2), source lens, reflectron 1, and reflectron 2 potentials were set at 25.03, 21.72, 9.65, 26.32, and 13.73 kV, respectively.

The $T_{\rm g}$ of the 6k tadpole-shaped polystyrene was determined using PerkinElmer Pyris DSC with a freon intercooler system. For the measurements, a sample of 8 mg was first heated from 15 to 125 °C at 10 °C/min under nitrogen atmosphere to erase the sample's thermal history. Then the sample was cooled down to 15 °C at 10 °C/min. The glass transition temperature was determined using a second heating scan from 15 to 125 °C at 10 °C/min using the Moynihan method. The absolute heat capacity was also determined over the same temperature range on heating after cooling at 30 °C/min using the step scan methodology with steps of 2 °C and isothermal holds of 0.8 min. Results reported are the average of three runs for the same sample. For comparison, similar measurements were performed on the linear analogue and the three-arm star precursor; results for these two materials are the average of individual runs for three different samples.

■ RESULTS AND DISCUSSION

The goal of this research was to develop a novel, efficient synthetic route for making tadpole-shaped polystyrene based on previous work for the synthesis of cyclic polystyrene, ^{24,25} 8-shaped polystyrene ²⁶ and asymmetric star polymers. ^{29–31} Living alkyllithium-initiated polymerization is one of the most reliable synthetic approaches to make polystyrenes with predictable molecular weights, narrow molecular weight distributions, and quantitative chain-end functionalities. 27,28,42-44 It is known from previous work that using an unsaturated, vinyl-substituted, alkyllithium initiator for living anionic polymerization can ensure that every α -chain end has a vinyl group. 43,45 Linking reactions of polymeric organolithium compounds with silvl halides are very efficient. 1,3 Utilizing this background, the reaction scheme for the synthesis of tadpoleshaped polystyrene shown in Scheme 1 was proposed. The first step was the preparation of the macromolecular linking agent (ω -methyldichlorosilylpolystyrene, (2). In the second step, α -4-pentenylpoly(styryl)lithium (3) reacted with the macromolecular linking agent to generate an asymmetric, three-arm, star polystyrene (4). In the final step, the α -4-pentenyl end groups were cyclized using the metathesis ring closure method to form the tadpole-shaped polystyrene (5).

Preparation of ω -Methyldichlorosilylpolystyrene (2). As shown in Scheme 1, sec-butyllithium was used as the initiator in benzene to polymerize styrene to generate a saturated, α -sec-butylpolystyrene linking agent (2). A base polymer sample was formed by quenching an aliquot of this PSLi (1) with methanol before reaction with excess methyltrichlorosilane (30-fold excess). The SEC chromatogram of sec-butyllithium-initiated polystyrene (Figure S1) shows a symmetric, monomodal distribution with $M_n = 1800$ g/mol $[M_n(\text{calcd}) = 2000 \text{ g/mol}]$, and $M_w/M_n = 1.08$. The concentration of poly(styryl)lithium was 3 wt % based on the work of Mays and co-workers, 30,31,46 because dimer formation occurs for reactions with methyltrichlorosilane if the concentration of poly(styryl)lithium is too high. An inverse

addition of the poly(styryl)lithium solution into a solution of excess methyldichlorosilane was also utilized to minimize dimer formation. Three freeze-dry cycles with benzene were carried out after the reaction to ensure that all excess methyltrichlorosilane was removed. The resulting macromolecular linking agent (2) in benzene was flame-sealed in an ampule which was then connected to the reactor for the next step of the reaction. The yield for this step is not available, since the macromolecular linking agent was sealed and used directly for the next step. However, based on the high efficiency of the silicon chloride linking reaction, ^{24–26,29,31} the yield should have been greater than 95%.

Synthesis of Asymmetric, Three-Arm, Star Polystyrene (4). The preparation of the asymmetric, three-arm, star polystyrene (4) is shown in Scheme 1. 5-Lithio-1-pentene was used as the initiator for polymerization of styrene in benzene. Five equivalents of THF were added to the initiator to facilitate the dissociation of the aggregates of this primary organolithium initiator and to increase the rate of initiation relative to propagation in order to obtain a narrow molecular weight distribution.^{27,33} THF was also useful to accelerate the rate of the chlorosilane linking reaction. The concentration of THF ([THF]/[RLi] = 5) used was decreased by 50% compared to previous work ([THF)]/[RLi] = 10)^{23–26} because the living chain end is quite sensitive to termination by THF.²⁷ An aliquot of the resulting α -4-pentenylpoly(styryl)lithium (3) was terminated by methanol as the base polymer for characterization, while the rest of PSLi, 3, α -4-pentenylpoly-(styryl)lithium] was reacted with the macromolecular linking agent (ω -methyldichlorosilylpolystyrene, 2). The SEC chromatogram of the α -4-pentenylpolystyrene (Figure S2) shows a symmetric, monomodal distribution with $M_{\rm n}$ = 1800 g/mol $[M_n(\text{calcd}) = 2000 \text{ g/mol}], M_w/M_n = 1.09. \text{ A 57 mol } \% \text{ excess}$ of PSLi chain ends relative to the silicon-chloride groups (Si-Cl) in the macromolecular linking agent was added to drive the reaction to completion. The linking process was allowed to proceed for 24 h. By reaction with ethylene oxide, the excess PSLi chains were converted to ω -hydroxyl- α -4-pentenylpolystyrene (6), which could be readily separated from the desired product, nonpolar asymmetric, three-arm, star polystyrene (4), by silica gel column chromatography. The yield based on the macromolecular linking agent (2) was 96%.

The SEC chromatogram of the asymmetric, three-arm, star precursor (4) (Figure 1) exhibited a symmetric, monomodal distribution, with $M_{\rm n}=5500~{\rm g/mol}~[M_{\rm n}({\rm calc})=5600~{\rm g/mol}],$ $M_{\rm w}/M_{\rm n}=1.09~{\rm and}~[\eta]=3.3~\pm~0.3~{\rm dL/g}.$ The $^{1}{\rm H}~{\rm NMR}$ spectrum (Figure 2a) of the linking reaction product exhibits characteristic vinyl resonances at δ 5.7 ppm (–CH=, H_a) and 4.9 ppm (=CH₂, H_b), respectively. The observed integration ratio (a/b) of 1.00:2.09 is consistent with the incorporation of vinyl groups in the three-arm star precursor (4). The multiplet between δ 0.5 and 0.8 ppm corresponds to the protons of sec-butyl methyl groups from the initiator (–CH₃, H_c). The integration ratio of this peak (6 H) relative to that of the vinyl protons (6 H) is 3.24:3.09, which is consistent with the proposed structure of asymmetric, three-arm, star polystyrene (4).

The MALDI-MS spectrum (Figure 3a) of the purified asymmetric, three-arm, star polystyrene (4) exhibits a clean, monomodal distribution, which shows that the excess linear chains with hydroxyl end groups have been completely removed by silica gel column chromatography. The theoretical monoisotopic mass based on the structure of the silver

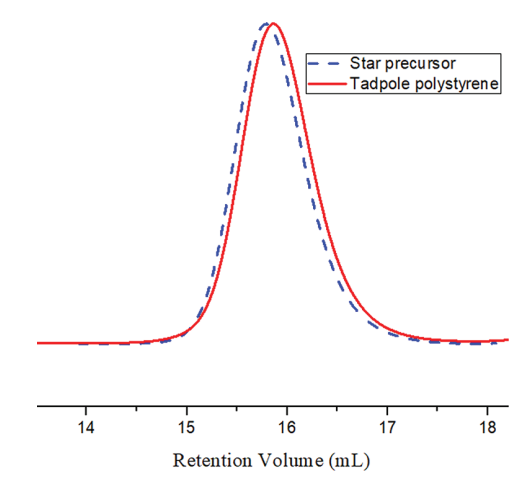


Figure 1. SEC chromatograms of purified asymmetric, three-arm, star precursor (4) (blue, dashed curve) and corresponding macrocyclic polystyrene (5) (red, solid curve).

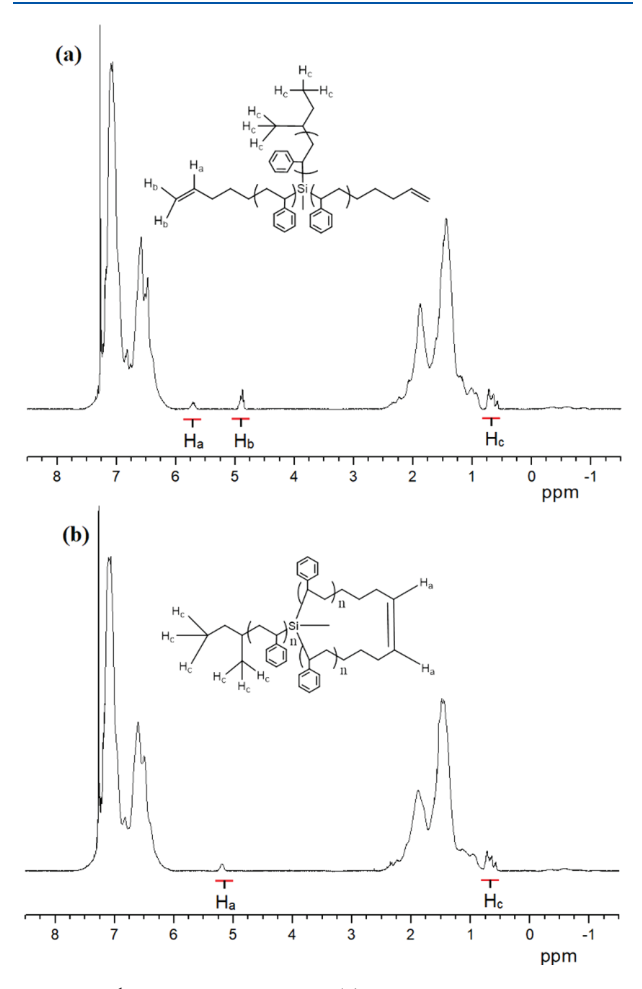


Figure 2. ¹H NMR spectra for (a) asymmetric, three-arm, star precursor (4). (b) for the tadpole-shaped polystyrene (5).

adducted 54-mer of the asymmetric, three-arm, star polystyrene (4) is 5964.58 Da [($C_{447}H_{462}Si+Ag$) $^{+}$: 57.07 ($C_{4}H_{9}$) + 2 × 69.07 ($C_{5}H_{9}$) + 43 (Si-CH $_{3}$) + 54 × 104.064 ($C_{8}H_{8}$) + 106.91 (Ag $^{+}$)] and the theoretical mass of the much more abundant, seventh isotopic peak (see Figures S3 and S4) of the

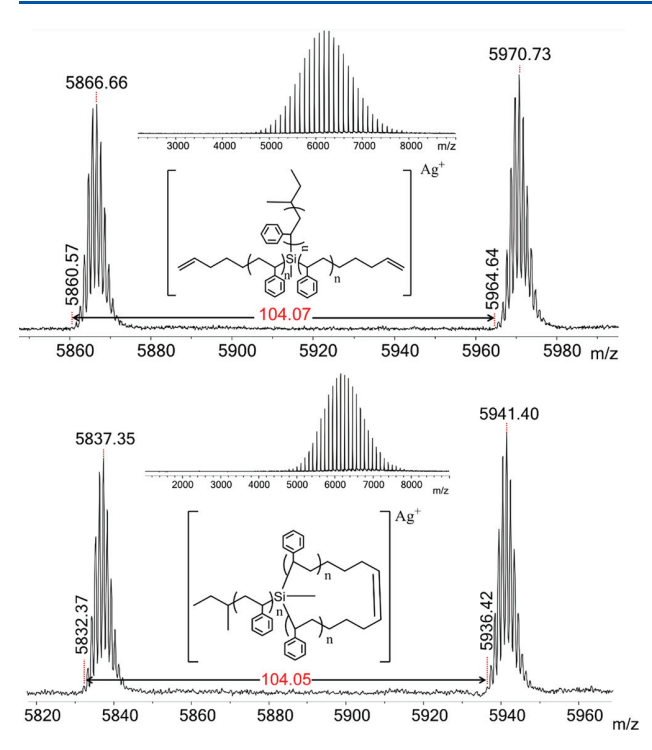


Figure 3. MALDI-MS spectra of (a) asymmetric, three-arm, star precursor (4) and (b) tadpole-shaped polystyrene (5).

same empirical formula is 5970.51. Both calculated values are consistent with the experimentally observed m/z values at 5964.64 and 5970.73, respectively. The distance between signals for neighboring oligomers is measured to be 104.07 Da, corresponding to the mass of a styrene unit. Therefore, the SEC, $^1\mathrm{H}$ NMR, and MALDI-MS characterizations are consistent and verify the structure of the asymmetric, three-arm, star polystyrene (4) with controlled molecular weight, narrow molecular weight distribution, and two vinyl chain ends

Synthesis of Tadpole-Shaped Polystyrene (5). The macrocyclization of polymeric precursors with telechelic α -and ω -divinyl groups using a metathesis catalyst has been shown to be very efficient. ^{23–26,47,48} On the basis of previous work, high dilution conditions were adopted to eliminate intermolecular chain extension. ^{24–26} The asymmetric, three-arm, star precursor (4) was treated with bis(tricyclohexylphosphine)benzylidene ruthenium(IV) chloride (Grubb's first generation catalyst) in methylene chloride for 40 h at 40 °C. The residual catalyst was removed by alumina column chromatography after exposure to air. The yield of the cyclized product (5) based on the three-arm precursor (4) was 81%.

The SEC chromatogram of the cyclization product (Figure 1) showed a symmetric, monomodal distribution with $M_{\rm n}=5500~{\rm g/mol},~M_{\rm w}/M_{\rm n}=1.09$ and $[\eta]=2.9\pm0.3~{\rm dL/g}.$ The slightly larger elution volume for the tadpole compared to that of the star precursor (Figure 1) indicates that the tadpole is slightly more compact than the star, as seen also by Tezuka et al. 19 The apparent difference in hydrodynamic volumes is smaller than the difference in hydrodynamic volumes between cyclic polymers and their linear analogs. 24,25,49,50 Since no MD simulations of the difference in hydrodynamic size of star and tadpole analogs have been previously published, such

simulations have been done here for comparison with the experimental results. Shown in Figure 4 are the probability

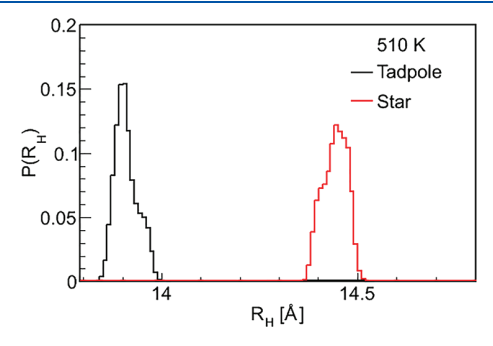


Figure 4. Probability distribution functions for hydrodynamic radii of the star and tadpole PS simulated using molecular dynamics of the pure melts at 510 K after 20 ns of equilibration.

distribution functions for the hydrodynamic radii $(R_{\rm H})$ for the star and tadpole PS as simulated for the pure melt at 510 K. (Additional plots for R_g and for the temperature of 550 K are shown in Figures S5-S7). The calculated ensemble average value $\langle R_{\rm H} \rangle$ for the tadpole is seen to be about 4% smaller than that of the star, so the hydrodynamic volume would be expected to be about 12% smaller. The hydrodynamic volumes $(V_{\rm H})$ corresponding to the peak positions in Figure 1 were calculated in the following way. The molecular weights of the linear chains corresponding to the two peak positions were found from the calibration curve created with linear PS standards. Then the infinite dilution diffusion coefficients corresponding to those molecular weights were interpolated from experimental light scattering data for linear PS in THF at 25 °C from Kok and Rudin. 51 From those diffusion coefficients, the hydrodynamic radii and thus the values of V_H corresponding to these peak positions were calculated. From the GPC data, $V_{\rm H}$ of the star chain is 11% larger than that for the tadpole. The results from the MD simulations thus agree very well with the experimental results, showing the small reduction in hydrodynamic volume that comes with the cyclization of the three-arm star to make the tadpole-shaped chain.

The ¹H NMR spectra of the cyclization product (Figure 2b) showed that the vinyl resonances at δ 4.9 ppm (-CH=, H_{a}) and δ 5.7 ppm ($=\text{CH}_2$, H_{c}) in the ¹H NMR spectrum of the precursor (Figure 2a) have disappeared, while a new internal vinyl proton resonance at δ 5.1 ppm is observed, as is expected for the tadpole-shaped polystyrene (5).²⁵ The integration ratio of the multiplet between δ 0.5 ppm to 0.8 ppm assigned to the sec-butyl methyl group protons (δ H) to the vinyl protons (δ 5.1, 2 H) is 3.28:1, which is in agreement with the expected structure (5).

MALDI-MS has proven to be the most definitive method to characterize and confirm the macrocyclic structure for metathesis ring closure products. ^{24–26} The mass spectrum of the tadpole-shaped polystyrene (5) (Figure 3b) exhibits a clean monomodal distribution. The absence of both higher and lower molecular weight impurities attests to the efficiency of this synthetic method. The theoretical monoisotopic mass based on the structure of the silver adducted 54-mer, tadpole-shaped polystyrene is 5936.55 Da [($C_{445}H_{458}Si + Ag$)⁺: 57.07 (C_4H_9) + 110.11 (C_8H_{14}) + 43 (Si-CH₃) + 54 × 104.064 (C_8H_8) + 106.91 (Ag^+)], and the theoretical mass of the most

abundant, sixth isotope (Figures S8 and S9) of the same empirical formula is 5941.48. Both theoretical values are in excellent agreement with the experimentally observed m/zvalues of 5936.42 and 5941.40. The reason why MALDI-MS is definitive for confirmation of the macrocyclic structure is that cyclization results in the elimination of an ethylene molecule from the asymmetric, three-arm, star precursor (4) during the cyclization. The mass difference between a given monoisotopic peak from the tadpole-shaped polystyrene (5) and the corresponding peak from the three-arm, star precursor (4) containing the same number of styrene repeating units should be m/z 28.0 (C₂H₄). Indeed, the monoisotopic peak for the 54-mer tadpole-shaped polystyrene is observed at m/z5936.42, while the monoisotopic peak of the corresponding 54-mer for the asymmetric, three-arm, star precursor (4) is observed at m/z 5964.64 (see Figure 3), giving a difference of m/z 28.22, which is consistent with the expected value for loss of an ethylene molecule during cyclization. Therefore, the MALDI-MS results are in agreement with SEC and ¹H NMR results, which demonstrate the efficiency of this ring closure reaction to produce a well-defined, tadpole-shaped polystyrene (5) with controlled molecular weight and narrow molecular weight distribution.

This synthetic methodology should work also for higher molecular weight tadpole molecules. Wang has explored the synthesis of macrocyclic polystyrenes with M of up to $36k^{24}$. That value is likely the attainable upper limit of molecular weight for the cyclic part of the molecule. As for the tail, which serves as a linking agent in our synthetic strategy, according to previous work by Fetters and Pennisi, 29 the upper limit can be up to 100k. This is dictated by the requirement that the functionalized end of the linking agent be able to "find" and react with the two arms to form the asymmetric 3-arm star precursor. The overall attainable M for the tadpole PS, based on this synthetic method, is therefore around 130k.

Physical Properties of 6k Tadpole-Shaped Polystyrene. Table 1 compares the values of T_g determined by DSC

Table 1. T_g 's for 6k Polystyrenes with Various Architectures

Molecular weight (g/mol) ^a	Architecture	Schematic	<i>T</i> _g (°C)
6000	Cyclic	$\langle \rangle$	98.9 ^b
5500	Tadpole		88.0°
6000	Linear	SS	85.3°
5500	3-arm star	3	76.3°
6000	4-arm star	X	77 ^b

^aMeasured using GPC with THF as eluent, uncertainty ±10%. ^bMeasured using TA Q200 DSC, heating and cooling rate of 10 K/min. ^cMeasured using PerkinElmer Pyris DSC, heating and cooling rate of 10 K/min.

for the three polymers in this study, as well as a 6k cyclic and 4-arm star analogs studied by He et al. The $T_{\rm g}$ of the linear 6k PS (synthesized by anionic polymerization) was measured to be 85.3 \pm 0.3 °C, and the $T_{\rm g}$'s of the 6k tadpole-shaped polystyrene and its three-arm star precursor synthesized here were determined to be 88.0 \pm 0.4 and 76.3 \pm 0.4 °C, respectively (Figure 5a). The effects of changes in the

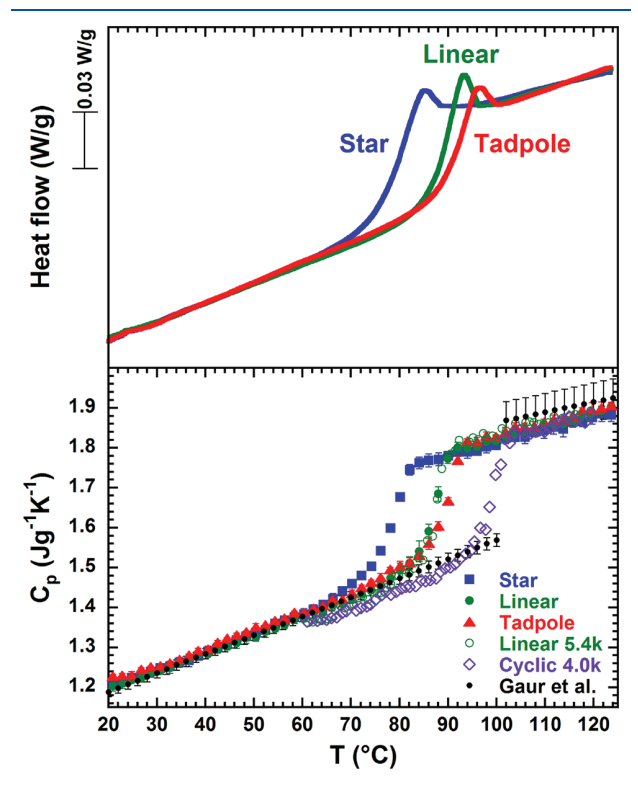


Figure 5. (a) (Top) DSC scans for the three-arm star precursor, tadpole, and linear analogue, performed on heating at 10 K/min after cooling at 10 K/min. (b) (Bottom) Absolute heat capacity for the three samples, along with results for a linear and cyclic polystyrene from Huang et al. ⁵³ and a compilation of results from the literature from Gaur and Wunderlich. ⁵⁵

architecture of the chains on $T_{\rm g}$ are apparent. As the number of chain ends decrease, and with it the free volume, the $T_{\rm g}$ increases. The larger number of chain ends in the star PS than in the linear PS introduces additional free volume, which markedly lowers $T_{\rm g}$ by 9 °C. After cyclization of the three-arm star polystyrene, the number of chain ends drops by 66%, and the T_g increases by 12 °C due to a reduction of free volume and becomes larger than that of the linear chain. The cyclic analog to the 6k linear PS chain of He et al. had a T_g of 98.9 $^{\circ}$ C. We had anticipated that the $T_{
m g}$ of the tadpole would be between the T_g 's of the cyclic chain and the linear chain of same overall molecular weight, and indeed that is what we see. In addition, the MD simulations show that at both 510 and 530 K, the tadpole density is 1% higher than the star precursor density, consistent with the higher $T_{\rm g}$ for the tadpole. The ordering of the T_g 's we see is also in line with the results of Monteiro and co-workers, 12 who found that the T_g of their TPS was between the T_g 's of their LPS analog and the interpolated value of $T_{\rm g}$ for a cyclic analog, all having overall molecular weights of 12k. However, in their case, the T_g of the

tadpole was closer to that for the cyclic than to that for the linear.

A quantitative comparison of the T_g 's from our work and those for similar structures reported in the literature is shown in Figure 6, where T_g is plotted as a function of the

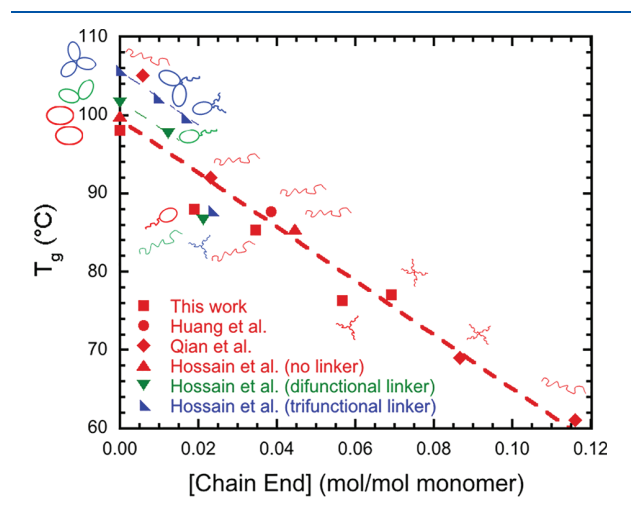


Figure 6. Summary of the variation of $T_{\rm g}$ with density of chain ends for the molecules considered in this work, set in the context of variations seen in other studies. To understand the $T_{\rm g}$ behavior for the star precursor and tadpole studied here, it is sufficient to consider the density of chain ends, whereas for some molecules from Monteiro et al. ¹⁵ with bulkier and stiffer junction points it is necessary to consider the junction point types as well.

concentration of chain ends. A linear relationship, as suggested by Fox and Flory, 52 is expected if the free volume arising from chain ends is the dominant factor determining $T_{\rm g}$. We note that although Ueberreiter and Kanig¹⁴ found a slightly better relationship with reciprocal T_g for small molecular weights, we plot the simpler relationship here for the purpose of clarity and because the difference in predictions from the two equations averages only 0.1 K in the regime we are interested in. The linear chains all follow the Fox and Flory linear relationship, with $T_{\rm g}$ decreasing with increasing free end concentration or decreasing molecular weight. In addition, our stars and tadpole also follow the same relationship, independent of structure, indicating that our junctions have no significant effect on $T_{\rm g}$. Similarly, a cyclic material previously studied⁵³ follows the same trend, as does a short four-arm star investigated by Archer and co-workers⁵⁴ and the linear chain from the study of Monteiro et al. 12 that does not contain a triazole junction. On the other hand, Monteiro's tadpoles, bicycles, and tricycles that contain triazole junctions have higher Tg's due to the constraints imposed by the junctions; this has been elegantly pointed out in their most recent work, with T_g shown to increase linearly with the number of constrained segments for structures with no chain ends. 15 Interestingly, two of the structures shown in Figure 6 (a linear chain and a three-arm star containing triazole junctions) also seem to follow the Fox and Flory relationship. Whether this is serendipitous or due to chain ends dominating in these materials is unclear. With the single atom junction used here, the explanation is more straightforward.

Additional insight from the thermal analysis is offered by consideration of the absolute heat capacity measurement, the results of which are shown in Figure 5b for the tadpole, its

three-arm precursor, and the linear counterpart, along with results from a low-molecular weight cyclic and linear polystyrene previously studied, and a compilation of literature data from Gaur and Wunderlich. ⁵⁵ In spite of the differences among the $T_{\rm g}$'s of the various materials, the absolute heat capacities are identical within the error of the measurements (±1%) and the same as for high molecular weight PS. The result suggests that the junctions in our molecules are not significantly impacting the pure material thermodynamics.

CONCLUSION

Well-characterized, tadpole-shaped polystyrene (5) with controlled molecular weight (6000 g/mol) and narrow molecular weight distribution has been prepared using a novel synthetic approach using a combination of anionic polymerization, silicon chloride linking chemistry, and metathesis ring closure. This unique and efficient methodology provides a tadpole-shaped polystyrene with only a single atom (Si) as junction point and provides product without high or low molecular weight impurities, as confirmed using SEC, ¹H NMR, and MALDI-ToF MS. No extensive purification methods (e.g., HPLC or fractionation) were required. This method could also be applicable to a variety of other polymers that can be synthesized using anionic polymerization. The glass transition temperature of the tadpole-shaped PS is 2.7 °C higher than that of its linear analog and 11.7 °C higher than that of the three-arm star analog, due to lower free volume with fewer chain ends. For these molecules in which the junction is a single atom, the change in $T_{\rm g}$ with architecture is adequately explained by considering self-plasticization by chain ends.

ASSOCIATED CONTENT

S Supporting Information

The Supporting Information is available free of charge on the ACS Publications website at DOI: 10.1021/acs.macromol.8b01384.

SEC chromatograms, experimental isotope patterns and theoretical isotope patterns for 54-mer asymmetric, three-arm, star polystyrene, and 54-mer tadpole-shaped polystyrene, and probability distribution functions for radius of gyration and hydrodynamic radius from MD simulations (PDF)

AUTHOR INFORMATION

Corresponding Author

*E-mail: mfoster@uakron.edu.

ORCID ®

Fan Zhang: 0000-0002-8890-9221

Chrys Wesdemiotis: 0000-0002-7916-4782

Mesfin Tsige: 0000-0002-7540-2050 Sindee L. Simon: 0000-0001-7498-2826 Mark D. Foster: 0000-0002-9201-5183

Notes

The authors declare no competing financial interest.

ACKNOWLEDGMENTS

We acknowledge assistance from Bojie Wang with SEC measurements and support from the University of Akron Research Foundation (MF) and the National Science Foundation (CHE-1808115 for C.W., CHE-1665284 for S.B. and M.T., and DMR-1610614 for S.L.S.).

REFERENCES

- (1) Bauer, B. J.; Fetters, L. J. Synthesis and Dilute-Solution Behavior of Model Star-Branched Polymers. *Rubber Chem. Technol.* **1978**, *51*, 406–436.
- (2) Endo, K. Synthesis and Properties of Cyclic Polymers. In *New Frontiers in Polymer Synthesis*, Kobayashi, S., Ed.; Springer: Berlin, 2008; pp 121–183.
- (3) Hadjichristidis, N.; Pitsikalis, M.; Pispas, S.; Iatrou, H. Polymers with Complex Architecture by Living Anionic Polymerization. *Chem. Rev.* **2001**, *101*, 3747–3792.
- (4) Roovers, J.; Toporowski, P. M. Relaxation by Constraint Release in Combs and Star-Combs. *Macromolecules* **1987**, *20*, 2300–2306.
- (5) Milner, S. T.; McLeish, T. C. B. Arm-Length Dependence of Stress Relaxation in Star Polymer Melts. *Macromolecules* **1998**, *31*, 7479–7482.
- (6) Larson, R. G. Combinatorial Rheology of Branched Polymer Melts. *Macromolecules* **2001**, *34*, 4556–4571.
- (7) Liu, B.; Narayanan, S.; Wu, D. T.; Foster, M. D. Polymer Film Surface Fluctuation Dynamics in the Limit of Very Dense Branching. *Macromolecules* **2013**, *46*, 3190–3197.
- (8) Wang, S.-F.; Jiang, Z.; Narayanan, S.; Foster, M. D. Dynamics of Surface Fluctuations on Macrocyclic Melts. *Macromolecules* **2012**, *45*, 6210–6219
- (9) He, Q.; Narayanan, S.; Wu, D. T.; Foster, M. D. Confinement Effects with Molten Thin Cyclic Polystyrene Films. *ACS Macro Lett.* **2016**, *5*, 999–1003.
- (10) Zhang, F.; He, Q.; Zhou, Y.; Narayanan, S.; Wang, C.; Vogt, B. D.; Foster, M. D. Anomalous Confinement Slows Surface Fluctuations of Star Polymer Melt Films. ACS Macro Lett. 2018, 7, 834–839
- (11) Zhang, L.; Elupula, R.; Grayson, S. M.; Torkelson, J. M. Major Impact of Cyclic Chain Topology on the T_g -Confinement Effect of Supported Thin Films of Polystyrene. *Macromolecules* **2016**, 49, 257–268
- (12) Hossain, M. D.; Lu, D.; Jia, Z.; Monteiro, M. J. Glass Transition Temperature of Cyclic Stars. ACS Macro Lett. 2014, 3, 1254–1257.
- (13) Gan, Y.; Dong, D.; Hogen-Esch, T. E. Effects of Lithium Bromide on the Glass Transition Temperatures of Linear and Macrocyclic Poly(2-vinylpyridine) and Polystyrene. *Macromolecules* 1995, 28, 383–385.
- (14) Ueberreiter, K.; Kanig, G. Self-Plasticization of Polymers. J. Colloid Sci. 1952, 7, 569–583.
- (15) Pipertzis, A.; Hossain, M. D.; Monteiro, M. J.; Floudas. Segmental Dynamics in Multicyclic Polystyrenes. *Macromolecules* **2018**, *51*, 1488–1497.
- (16) Wang, S.-F.; Yang, S.; Lee, J.; Akgun, B.; Wu, D. T.; Foster, M. D. Anomalous Surface Relaxations of Branched-Polymer Melts. *Phys. Rev. Lett.* **2013**, *111*, 068303.
- (17) Doi, Y.; Takano, A.; Takahashi, Y.; Matsushita, Y. Melt Rheology of Tadpole-Shaped Polystyrenes. *Macromolecules* **2015**, *48*, 8667–8674.
- (18) Beinat, S.; Schappacher, M.; Deffieux, A. Linear and Semicyclic Amphiphilic Diblock Copolymers. 1. Synthesis and Structural Characterization of Cyclic Diblock Copolymers of Poly(hydroxyethyl vinyl ether) and Linear Polystyrene and Their Linear Homologues. *Macromolecules* 1996, 29, 6737–6743.
- (19) Oike, H.; Uchibori, A.; Tsuchitani, A.; Kim, H.-K.; Tezuka, Y. Designing Loop and Branch Polymer Topology with Cationic Star Telechelics through Effective Selection of Mono- and Difunctional Counteranions. *Macromolecules* **2004**, *37*, 7595–7601.
- (20) Li, H.; Debuigne, A.; Jérome, R.; Lecomte, P. Synthesis of Macrocyclic Poly(ε -caprolactone) by Intramolecular Cross-Linking of Unsaturated End Groups of Chains Precyclic by the Initiation. *Angew. Chem., Int. Ed.* **2006**, 45, 2264–2267.
- (21) Shi, G.-Y.; Tang, X.-Z.; Pan, C.-Y. Tadpole-Shaped Amphiphilic Copolymers Prepared via RAFT Polymerization and Click Reaction. *J. Polym. Sci., Part A: Polym. Chem.* **2008**, *46*, 2390–2401.
- (22) Doi, Y.; Ohta, Y.; Nakamura, M.; Takano, A.; Takahashi, Y.; Matsushita, Y. Precise Synthesis and Characterization of Tadpole-

Shaped Polystyrenes with High Purity. *Macromolecules* **2013**, 46, 1075–1081.

- (23) Wang, S. F. Synthesis and Characterization of Surface Relaxations of Macrocyclic Polystyrenes and Interfacial Segregation in Blends with Linear Polystyrenes. Ph.D. Dissertation, University of Akron, 2011.
- (24) Quirk, R. P.; Wang, S.-F.; Foster, M. D.; Wesdemiotis, C.; Yol, A. M. Synthesis of Cyclic Polystyrenes Using Living Anionic Polymerization and Metathesis Ring-Closure. *Macromolecules* **2011**, 44, 7538–7545.
- (25) He, Q.; Yol, A. M.; Wang, S.-F.; Ma, H.; Guo, K.; Zhang, F.; Wesdemiotis, C.; Quirk, R. P.; Foster, M. D. Efficient Synthesis of Well-Defined Cyclic Polystyrenes using Anionic Polymerization, Silicon Chloride Linking Chemistry and Metathesis Ring Closure. *Polym. Chem.* **2016**, *7*, 5840–5848.
- (26) He, Q. M.; Mao, J.; Wesdemiotis, C.; Quirk, R. P.; Foster, M. D. Synthesis and Isomeric Characterization of Well-Defined 8-Shaped Polystyrene Using Anionic Polymerization, Silicon Chloride Linking Chemistry, and Metathesis Ring Closure. *Macromolecules* **2017**, *50*, 5779–5789.
- (27) Hsieh, H. L.; Quirk, R. P. Anionic Polymerization: Principles and Practical Applications; Marcel Dekker: New York, 1996.
- (28) Quirk, R. P.; Pickel, D. L. Controlled End-Group Functionalization (including Telechelics). In *Polymer Science: A Comprehensive Reference*, Matyjaszewski, K., Møller, M., Eds.; Elsevier BV: Amsterdam, 2012; Vol. 6, pp 351–412.
- (29) Pennisi, R. W.; Fetters, L. J. Preparation of Asymmetric 3-Arm Polybutadiene and Polystyrene Stars. *Macromolecules* **1988**, *21*, 1094–1099.
- (30) Mays, J. W. Synthesis of "Simple Graft" Poly(Isoprene-g-Styrene) by Anionic Polymerization. *Polym. Bull.* **1990**, 23, 247–250.
- (31) Uhrig, D.; Hong, K.; Mays, J. W.; Kilbey, S. M.; Britt, P. F. Synthesis and Characterization of an ABC Miktoarm Star Terpolymer of Cyclohexadiene, Styrene, and 2-Vinylpyridine. *Macromolecules* **2008**, *41*, 9480–9482.
- (32) Tezuka, Y.; Komiya, R. Metathesis Polymer Cyclization with Telechelic Poly(THF) Having Allyl Groups. *Macromolecules* **2002**, *35*, 8667–8669.
- (33) Quirk, R. P.; Ma, J.-J. Dilithium Initiators Based on 1,3-bis(1-Phenylethenyl)benzene. Tetrahydrofuran and Lithium sec-Butoxide Effects. *Polym. Int.* **1991**, *24*, 197–206.
- (34) Morton, M.; Fetters, L. J. Anionic Polymerization of Vinyl Monomers. *Rubber Chem. Technol.* **1975**, 48, 359–409.
- (35) Hadjichristidis, N.; Iatrou, H.; Pispas, S.; Pitsikalis, M. Anionic Polymerization: High Vacuum Techniques. *J. Polym. Sci., Part A: Polym. Chem.* **2000**, *38*, 3211–3234.
- (36) Uhrig, D.; Mays, J. W. Experimental Techniques in High-vacuum Anionic Polymerization. *J. Polym. Sci., Part A: Polym. Chem.* **2005**, 43, 6179–6222.
- (37) Gilman, H.; Cartledge, F. K. The Analysis of Organolithium Compounds. J. Organomet. Chem. 1964, 2, 447–454.
- (38) Watkins, E. K.; Jorgensen, W. L. Perfluoroalkanes: Conformational Analysis and Liquid-State Properties from Ab Initio and Monte Carlo Calculations. *J. Phys. Chem. A* **2001**, *105*, 4118–4125.
- (39) Tatek, Y. B.; Tsige, M. Structural Properties of Atactic Polystyrene Adsorbed onto Solid Surfaces. *J. Chem. Phys.* **2011**, *135*, 174708.
- (40) Plimpton, S. Fast Parallel Algorithms for Short-Range Molecular Dynamics. *J. Comput. Phys.* **1995**, *117*, 1–19.
- (41) Moynihan, C. T.; Easteal, A. J.; Bolt, M. A.; Tucker, J. Dependence of the Fictive Temperature of Glass on Cooling Rate. *J. Am. Ceram. Soc.* **1976**, *59*, 12–16.
- (42) Quirk, R. P. Anionic Polymerization of Nonpolar Monomers. In *Polymer Science: A Comprehensive Reference*, Matyjaszewski, K., Møller, M., Eds.; Elsevier BV: Amsterdam, 2012; Vol. 3, pp 559–590.
- (43) Quirk, R. P.; Jang, S. H.; Kim, J. Recent Advances in Anionic Synthesis of Functionalized Elastomers Using Functionalized Alkyllithium Initiators. *Rubber Chem. Technol.* **1996**, *69*, 444–461.

(44) Anionic Polymerization: Principles, Practice, Strength, Consequences and Applications; Hadjichristidis, N., Hirao, A., Eds.; Springer: Tokyo, 2015.

- (45) Takano, A.; Furutani, T.; Isono, Y. Preparation of a Polystyrene Macromonomer with a Novel Anionic Initiator Containing an Olefinic Vinyl Group. *Macromolecules* **1994**, *27*, 7914–7916.
- (46) Lee, C.; Gido, S. P.; Pitsikalis, M.; Mays, J. W.; Tan, N. B.; Trevino, S. F.; Hadjichristidis, N. Asymmetric Single Graft Block Copolymers: Effect of Molecular Architecture on Morphology. *Macromolecules* 1997, 30, 3732–3738.
- (47) Bielawski, C. W.; Benitez, D.; Grubbs, R. H. An "Endless" Route to Cyclic Polymers. *Science* **2002**, 297, 2041–2044.
- (48) Hayashi, S.; Adachi, K.; Tezuka, Y. An Efficient Route to Cyclic Polymers by ATRP–RCM Process. *Chem. Lett.* **2007**, *36*, 982–983.
- (49) Roovers, J.; Toporowski, P. M. Synthesis of High Molecular Weight Ring Polystyrenes. *Macromolecules* **1983**, *16*, 843–849.
- (50) Laurent, B. A.; Grayson, S. M. Synthetic Approaches for the Preparation of Cyclic Polymers. *Chem. Soc. Rev.* **2009**, *38*, 2202–2213.
- (51) Kok, C. M.; Rudin, A. Relationship between The Hydrodynamic Radius and the Radius of Gyration of a Polymer in Solution. *Makromol. Chem., Rapid Commun.* **1981**, *2*, 655–659.
- (52) Fox, T. G.; Flory, P. J. Second-Order Transition Temperatures and Related Properties of Polystyrene. I. Influence of Molecular Weight. *J. Appl. Phys.* **1950**, *21*, 581–591.
- (53) Huang, D. H.; Simon, S. L.; McKenna, G. B. Chain Length Dependence of the Thermodynamic Properties of Linear and Cyclic Alkanes and Polymers. *J. Chem. Phys.* **2005**, 122, 084907.
- (54) Qian, Z.; Minnikanti, V. S.; Sauer, B. B.; Dee, G. T.; Kampert, W. G.; Archer, L. A. Surface Tension of Polystyrene Blends: Theory and Experiment. *J. Polym. Sci., Part B: Polym. Phys.* **2009**, *47*, 1666–1685
- (55) Gaur, U.; Wunderlich, B. Heat-capacity and Other Thermodynamic Properties of Linear Macromolecules 5. Polystyrene. *J. Phys. Chem. Ref. Data* **1982**, *11*, 313–325.